*Istraživanja i projektovanja za privredu*
*ISSN 1451-4117*
*DOI:10.5937/jaes0-51405*
*www.engineeringscience.rs*

iipp publishing

***Journal of Applied Engineering Science***
*Vol. 22, No. 4, 2024*
*Original Scientific Paper*
*Paper number: 22(2024)4, 1239, 761-771*

# *ANALYZE THE PERFORMANCE OF HORNS WITH COMPLEX WORKING SURFACES USED IN ULTRASONIC WELDING OF CAR TURN SIGNALS*

***Ngo Nhu Khoa[1], Dang Anh Tuan[2], Nguyen Dinh Ngoc[2]****

*[1] Thai Nguyen University of Technology, Faculty of Mechanical Engineering, Department of Industry System, Thai Nguyen city, Vietnam*
*[2] Thai Nguyen University of Technology, Faculty of International Training, Department of Mechanical Engineering, Thai Nguyen city, Vietnam*
** ngocnd.cenis@tnut.edu.vn*

*Ultrasonic plastic welding technology has been widely applied in practice. Welding horn design is one of the important tasks. Many studies have presented this problem. However, most of these studies are only interested in face profiles that are flat or have symmetrical profiles. Meanwhile, ultrasonic welding horns with complex working surfaces receive little attention. This research presented the design of an ultrasonic horn with a complex working surface. Moreover, the influence of the slot width in the horn, an important design parameter, on the performance of the designed horn was considered. The finite element method was used for modal and harmonic analysis. The performance of the design was assessed through criteria that are the uniformity of amplitude, the distribution of the greatest stress at points on the working surface, and closed to the target frequency. A new parameter, namely Displacement unevenness (a), was proposed to evaluate the unevenness amplitude in the working surface of the horn. Effects of three alternative slot structures width corresponding values of 12 mm, 17 mm and 20 mm, denoted by B12, B17, and B20 respectively were carried out. The results showed that the B12 and B17 designs have natural frequencies close to the target frequency of the welding machine, while the natural frequency of the B20 design is far from the target one. The B12 and B17 designs also produce an unevenness amplitude smaller than those of the B20 design. The model showing the relationship between design parameters and the required criteria must be further developed. Additionally, this result can be said for the design guidelines not fully available in the literature.*

*Keywords: ultrasonic welding, displacement unevenness, modal analysis, harmonic analysis, car turn signals*

## *1 INTRODUCTION*

Ultrasonic welding is a pressure welding process, using the mechanical energy of ultrasonic vibrations to generate the local plastic deformation at the joint surface. This process causes the elements of the welded parts to diffuse, penetrate each other and bond together to form a weld [1-3]. In recent decades, ultrasonic welding technology has been widely used in industry to weld structures made of a variety of materials such as Carbon-fiber reinforced polymer, plastics, metallic materials, etc. It is widely used in aviation, automobile, household appliances, food, electronics, medicine. The factors that make it attractive to different industries as mentioned above are because of its valuable properties. These ones are able to weld metals with low resistance; can weld different metals, weld metal to non-metal, weld plastic, weld bone, allowing to weld details with thickness ratio up to 1:1000; consumes little energy; ease of automation [4-6]. The welding time of this technology is normally less than 1 second. Usually, the basic components of an ultrasonic welding system are power supply, transducer, booster, horn, actuator, and fixture [7-9]. Among these parts, the horn is a very important component which connects the welded parts and converts the ultrasonic waves generated from transducer. The design characteristics of the horn can directly impact on the quality of the weld. The horn is designed to resonate at the desired frequency and vibrate in longitudinal mode [10-12]. In the past, the trial-and-error method was often used to design the horn. Recently, thanks to the development of information technology, the finite element method (FEM), has been widely applied by researchers. Cardoni et al. [13] studied the performance of an ultrasonic block welding horn using finite element analysis (FEA) in which the uniform vibration amplitude on the working surface is a design requirement to improve the performance of the block horn by introducing the slots along the length horns. The geometric dimensions of the slots in the block horn design are determined to achieve the maximum value of vibration amplitude using FEA. Graham et al. [14] presented the results of modal analysis of ultrasonic block horns using Electronic Speckle Pattern Interferometry. The horn is modeled and analyzed using the FEM. Frequency response function data is obtained from ESPI data by monitoring the electrical signal. The authors concluded that the results from the modal analysis are in good agreement with the FEA results. Lucas et al. [15] redesigned the ultrasonic block welding head to improve the performance of the welding head. Modal analysis was performed on the block weld head using FEA. Two laser-based vibration measurement techniques, laser Doppler velocimetry and electron speckle pattern interferometry, were used to experimentally measure the natural vibration frequency of the welding tip. Kim et al. [16] studied the effect of slot size on the design of tube and weld horn to achieve high amplitude uniformity using Design of Experiments. The natural frequency and displacement amplitude of the working surface are analyzed by FEM. The results showed that the width and length slots have a significant influence on amplitude uniformity. Recently Rani [17] developed computational models for different

configurations of solid welding horns used in ultrasonic plastic welding to determine the dynamic characteristics. Based on the previously analyses, it can be said that there have been studies on horn design to increase productivity and improve weld quality. However, the results of these studies only focus on the design of welding horns with simple welding profiles. Meanwhile, there have been few studies focusing on the design of welding heads with complex working surface having complicated profiles.

In order to contribute to filling the scientific gap mentioned above, in this study research dealing with the design of the horn with complex working surface will be conducted. The results in the literature reveal that the amplitude of working surface increase with increasing in slot width [18-20], the influence of slot width on the performance of the horn will be analyzed. The performance of the horn is evaluated through three factors. First, vibration of the working surface on the horn tip should be as uniform as possible. Second, the nature frequency of longitudinal mode of the designed horn should be closed to the target frequency emitted by the transducer. Finally, the maximum stress generated inside the horn body should be small, and lower than the endurance limit to prevent damage to the horn due to fatigue. Modal analysis and harmonic analysis will be used through the FEA model to be evaluated.

## 2 MATERIALS AND METHODS

The horn needed to design is used for welding a pair of cars turn signals which made of Acrylonitrile Butadiene Styrene, or ABS materials. In order to satisfy the requirements of plastics welding, the horn materials should possess the good fatigue strength, excellent acoustic properties, and good surface hardness. Among the available ones, Aluminium Alloy of Al-6061-T6 can meet the mentioned demands. The details of this materials are presented in Table 1.

Table 1. Properties of aluminum alloy (Al-6061-T6) [9]

| Young' modulus (GPa) | Poisson's ratio (υ) | Density (kg/m$^3$) |
|---|---|---|
| 70 | 0.33 | 2700 |

The horn designed in this study is for ultrasonic welding of a pair of car turn signals showed in Fig 1 in which the upper part is directly connected by the working surface of the horn, while the below part is kept in the anvil. The required horn has the shape in the form of a block to satisfy the dimensions of welded parts. To transmit energy into the welding area, the working surface of the horn must entirely cover the working surface of the upper part of the weld (Fig 1.a). A 3D scanning device was used to capture the three-dimensional profile of obve part of the car turn signal. The collected data were exported to reverse engineering software for implementation. A proposed CAD model of the designed horn can be seen in Fig 2.


Fig. 1. Products of car turn signals for ultrasonic welding (a) upper part and (b) below part

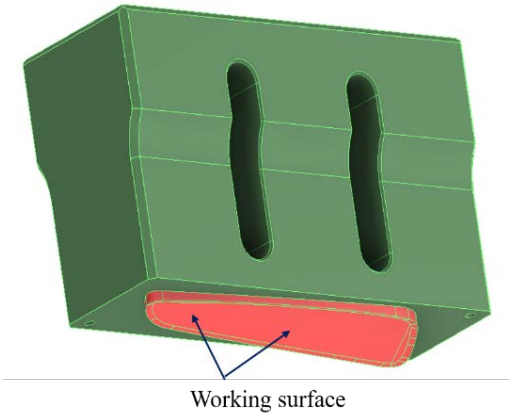


Fig. 2. A CAD model of the designed block horn with complex working surface

The width and thickness are selected due to those of the workpieces, while the length is dependent on the mechanical properties of horn materials such as density and Young's modulus as Equation (1) [18].

$$\lambda = \frac{c}{f} = \frac{1}{\mathrm{f}}\sqrt{\frac{\mathrm{E}}{\rho}} = 2l \quad (1)$$

Where,

c - Velocity of sound (m/sec)

E – Modulus elasticity of the horn material (Gpa)

ρ - Density of the horn material (kg/m$^3$)

*l* – The horn length (mm)

$\lambda$ - Wavelength of mechanical vibration (μm)

*f* – Frequency of vibration (Hz)

The horn length should be an integer number of half the wavelength of the mechanical vibration produced by the transducer. In this study, half the wavelength is taken as the height of the block horn. The working frequency of the welder is selected as 20 kHz. The speed of sound through aluminum alloy (Al-6061-T6) is calculated as follows:

$$\mathrm{c} = \sqrt{\frac{E}{\rho}} = 5091.75 \text{ m/s}$$

the wavelength of mechanical vibration,

$$\lambda = \frac{c}{f} = \frac{5091.75}{20000} = 0.254 \text{ m}$$

$$2\mathrm{l} = 0.254 \text{ m}$$

This gives,

$$\mathrm{l} = \frac{\lambda}{2} = 0.127\ m$$

Hence, the horn length is theoretically found to be 0.127 m. According to the recommendation given by [19], the actual length of the horn should be varied 10-15% of the length previously determined. In this design the length of the horn of 115 mm (*l*) is adopted. The highest distance in the working surface to the bottom face of the horn ($h_0$) is chosen of 4 mm based on our experiences. The horn thickness ($t_2$) and width (b) depend on the corresponding dimensions of the welded parts. The width of the slot (s), the width of each rod ($l_1$) can be considered the variables herein. Morevoer, in order to magnify the working surface amplitude, a step located at the distance of $h_1$ is adopted. The magnification factor is determined by the cross-section areas between the upper surface and the lower surface. The details of dimensional information of the designed horn are listed in Table 2 and in Fig 3.

Table 2. The basic dimensions of the designed horn

| *l* (mm) | b (mm) | $t_1$ (mm) | $t_2$, (mm) | r, (mm) | $h_1$ (mm) | $h_0$ (mm) |
|---|---|---|---|---|---|---|
| 115 | 200 | 75 | 63 | 31 | 45 | 4 |

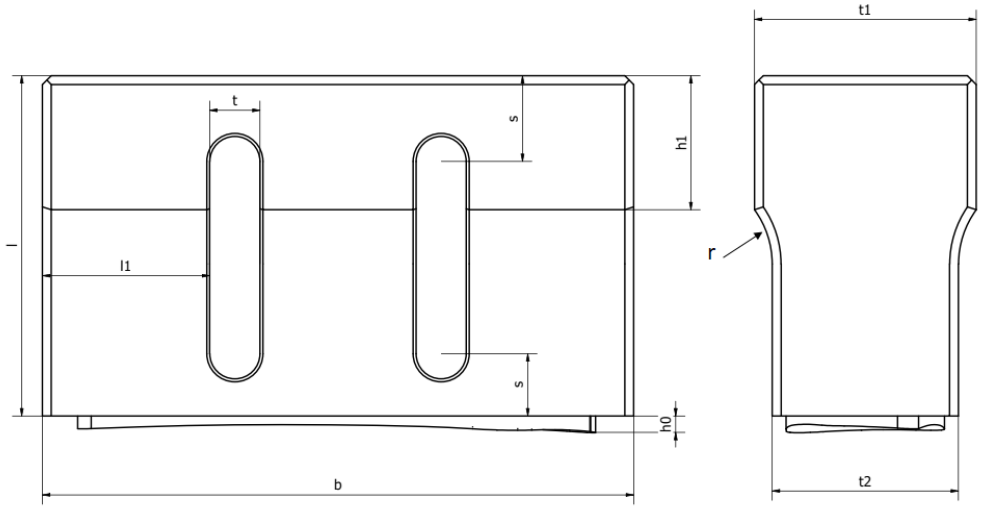


Fig. 3. Basic dimensions of complex profile ultrasonic welding horn

The dynamic characteristics of the ultrasonic block horn were studied by FEM using the commercial software ABAQUS. The FEM model meshes using a 10-node C3D10 element with a mesh size of 4 mm. This is a 4-sided quadratic element suitable for 3D design with variable cross-section and complex profile with 3 degrees of freedom at each node. The selected types of elements are capable of representing different forms of damage such as creep, stress, plasticity, super elasticity, and large deformation. To achieve the optimal geometric dimension of the horn, several dimensional parameters should be investigated simultaneously. These include slot width (t), slot length (l), distance from the top to the slot (s), upper body thickness ($t_1$), lower body thickness ($t_2$), and radius fillet angle (Fig 2). However, in the current study, the influence of slot width is only focused on because this parameter is recommended as having a significant influence on welding horn design [20, 21]. The displacement in the working surface of the ultrasonic horn can be uniform if introducing the small slots along to the horn length [19, 22, 23]. In this section the importance of slotting in the block horn with the width which is relatively large will be emphasized one more time.

## *3 RESULTS AND DISCUSSION*

The comparison in term of the regularity of the working surface between two designs without and with slots will be carried out. The first one is a block horn without introducing slots and the second is the one including slots. There are three criteria used to show the performance are the longitudinal natural frequency, the displacement of working surface of the horn, and the maximum stress in the horn. In this case the longitudinal natural frequency referring to the resonant frequency should be close the target frequency or the working frequency of the welder, 20kHz. For the design without slots, thanks to the modal analysis, it is observed that the longitudinal vibration model is 18568 Hz as shown in Fig 4. The percentage error compared to the target frequency is 7.6%. The preceding and the next vibration modes are bending and torsion which have the frequency of 18972 Hz and 17362 Hz respectively (Fig 5). The big value of the frequency difference between the natural and targeting is attributed to the coupling of the transverse and longitudinal modes.

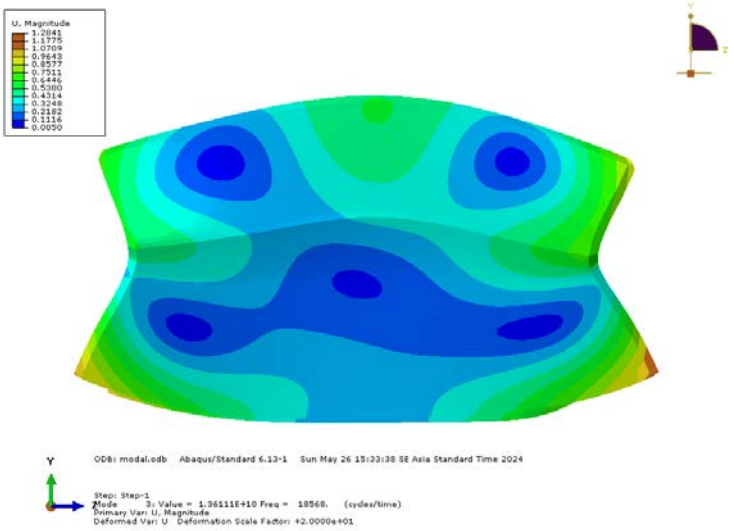


Fig. 4. Longitudinal mode of the block horn without slots

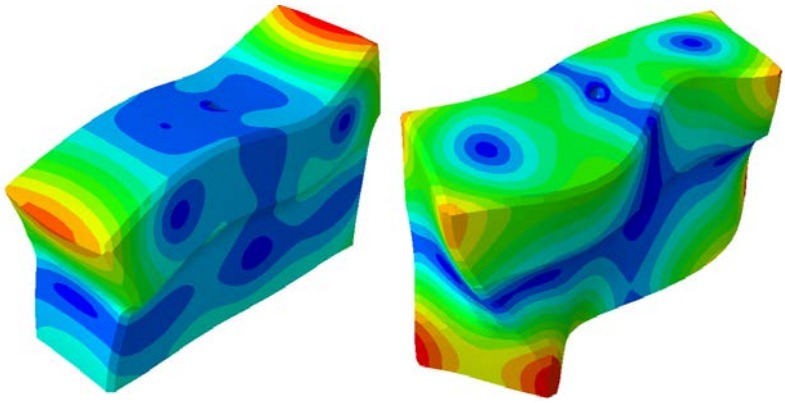

Fig. 5. Bending (a) and torsional (b) mode of the initial design

A value of displacement of 10 μm at the end of booster considered as input of the block horn is imposed to conduct the harmonic analysis. The details of imposing boundary conditions will be clearly described later. This is the given displacement value assumed to be amplified from the transducer of the welder. The natural frequency of 18568 Hz belonging to the longitudinal mode is applied to determine the stress and the displacements in the working surface of the block horn. Fig 6 shows the color chart referring the displacements on the points at the working surface. It is observed that the variation of working surface displacement is significantly different. This may be due to the appearance of the Poison effect. This means that addition to longitudinal vibration mode, the block horn also transversely vibrates [3, 9]. Hence, the displacements on the working surface of the block horn are not uniform.

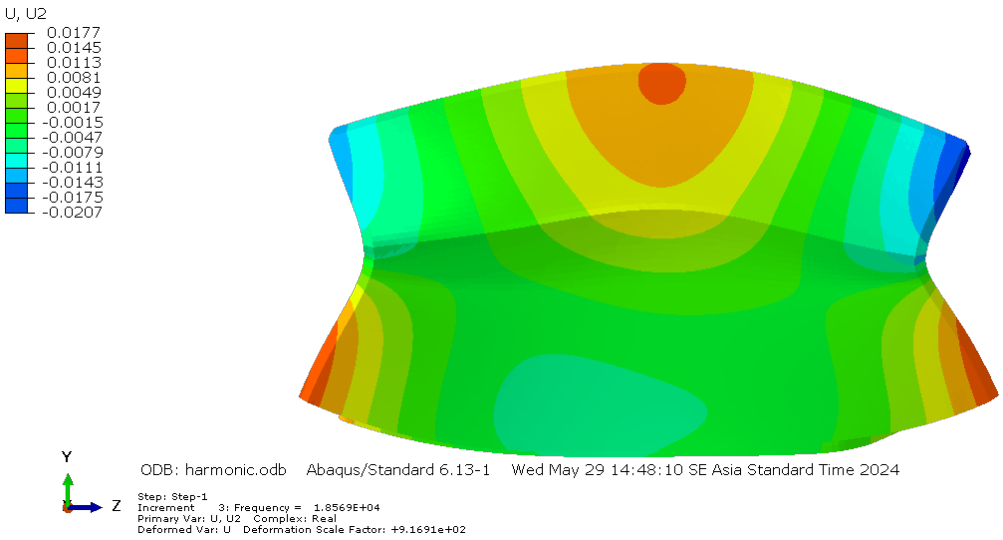


Fig. 6. Displacement analysis of the longitudinal vibration mode of the initial design

To minimize the variation of working surface displacements because of the interaction between the desired and undesirable modes as mentioned above, the slots are created along the horn length. In this section of this paper, the slotted welding horn design is designed and analyzed in which the effect of width slots on the dynamics properties of the horn. Two types of analysis commonly performed are modal and harmonic analysis. The former is used to determine the natural frequency and vibration mode of the welding horn. The design of the horn is tuned until the longitudinal mode at the resonant frequency obtained according to the design error of less than 10%. This is done by preliminary analysis. After receiving the longitudinal mode shape in the frequency range of the machine, harmonic analysis is performed. In the harmonic analysis, the displacement amplitude at the output face of the welding horn and the induced von Mises stress in the welding horn are predicted by applying boundary conditions. Three configurations of the horn design corresponding to three different values of the width slot such as 12 mm, 17mm, and 20mm are considered. The dimension detail of each design is shown in Table 2 where except for the width slots, other dimensions are similar to all horn configurations. In order to simplify, three designs with three slot widths of 12 mm, 17 mm, and 20 mm will be abbreviated as T12, T17, and T20 respectively.

### *3.1. Modal analysis*

It is noticed that the designed horn is asseblied to the booster by a screw. However, in this case it is not taken into account of the CAD model due to simplifying the model during simulation. In addition, the influence of the screw on the numerical results can be approximated through the use of the reasonable boundary conditions imposed at the screw installation location as shown in Figure 8 [24]. Mode extractions are carried out between the frequency range

of 16-22 kHz. With the given frequency range, the extracted modes are analyzed. The eigenvalue extraction (natural frequencies) using the Lanczos method. In addition to the longitudinal modes, the appearance of bending and torsional modes are observed. However, only the longitudinal mode Fig of the designs is showed. The modal analysis of the T12 design presented in Fig 7 shows that the natural frequency in longitudinal mode in this case is found to be 20313 Hz which is different from the frequency excited by transducer-booster (20000 Hz) by 1.6%. The natural frequencies in the longitudinal mode of T17 and T20 are 20033 Hz and 18631 Hz respectively. These values in turn are different from the target frequency by 0.2% and 6.8%. Therefore, it is said that the natural frequency given by the T20 design is not able to match the excited frequency and is difficult to resonate uniformly at the working surface profile of the horn. On the other hand, the design of T12 and T17 give similar results of matching to target frequency. In term of separation frequency between turned mode and the next ones for three designs can be observed in Table 2. It can be concluded that the design T20 gives less isolation of frequency between the longitudinal mode and other.

Table 2. The natural and isolation frequency of three design

| | Design of T12 | | Design of T17 | | Design of T20 | |
|---|---|---|---|---|---|---|
| | Frequency (kHz) | Isolation frequency (kHz) | Frequency (kHz) | Isolation frequency (kHz) | Frequency (kHz) | Isolation frequency (kHz) |
| Torsion | 19421 | 892 | 18897 | 1135 | 18518 | 113 |
| Longitudinal | 20313 | | 20032 | | 18631 | |
| Bending | 20989 | 676 | 20675 | 643 | 19056 | 425 |

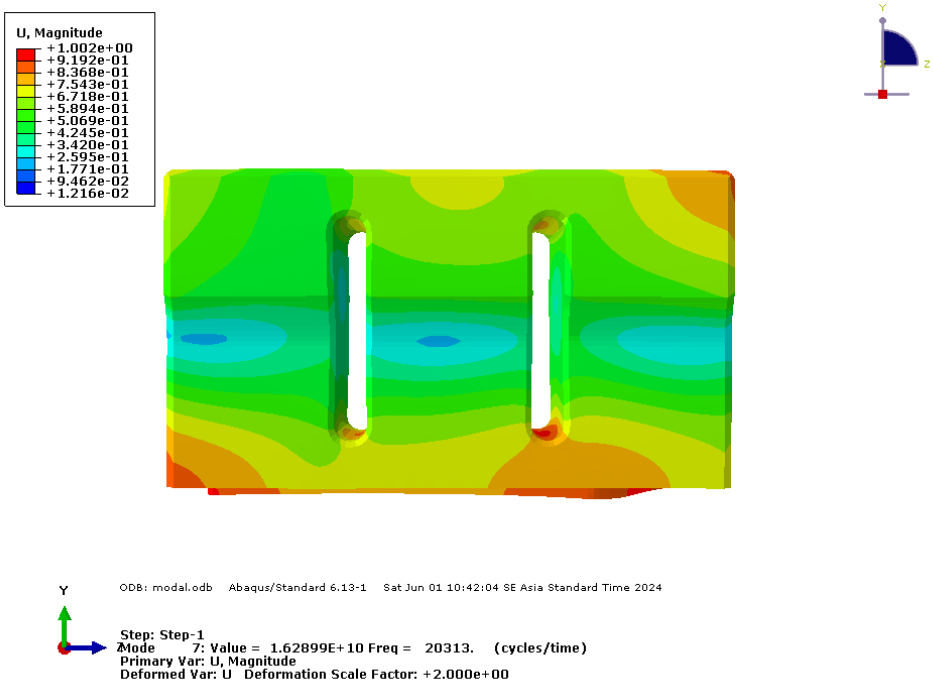


Fig. 7. Modal analysis of T12 design

### *3.2. Harmonic analysis*

The boundary conditions applied to this step are imposing the bolt position in the upward face connecting to the booster. A displacement value of 10 μm is applied. The application process of the boundary conditions can be seen in Fig 6.

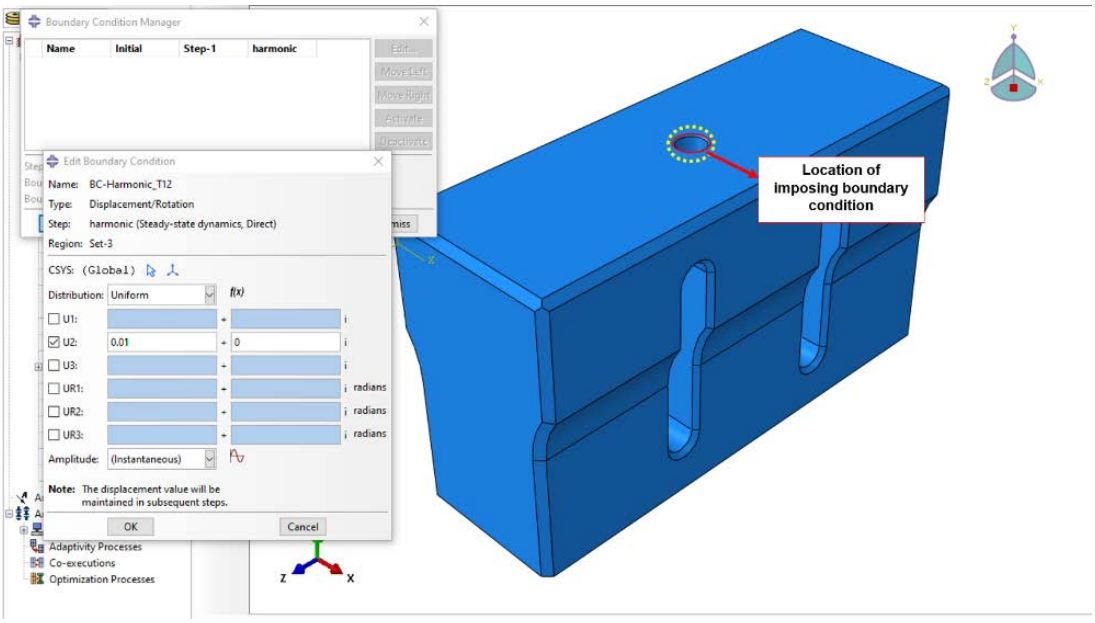


Fig. 8. Description of imposing boundary conditions for harmonic analysis

In this step, the extracted vibration modes in the modal analysis are utilized to evaluate the performance of the proposed designs. The amplitude uniformity of the working surface profiles and maximum stress generated in the horn body is taken into account. Fig 7 shows the color chart referring to the absolute displacement values of the horn body in the T12 design. It is observed that the points in the above part displace upward and the points in the below parts move downward in the longitudinal direction.

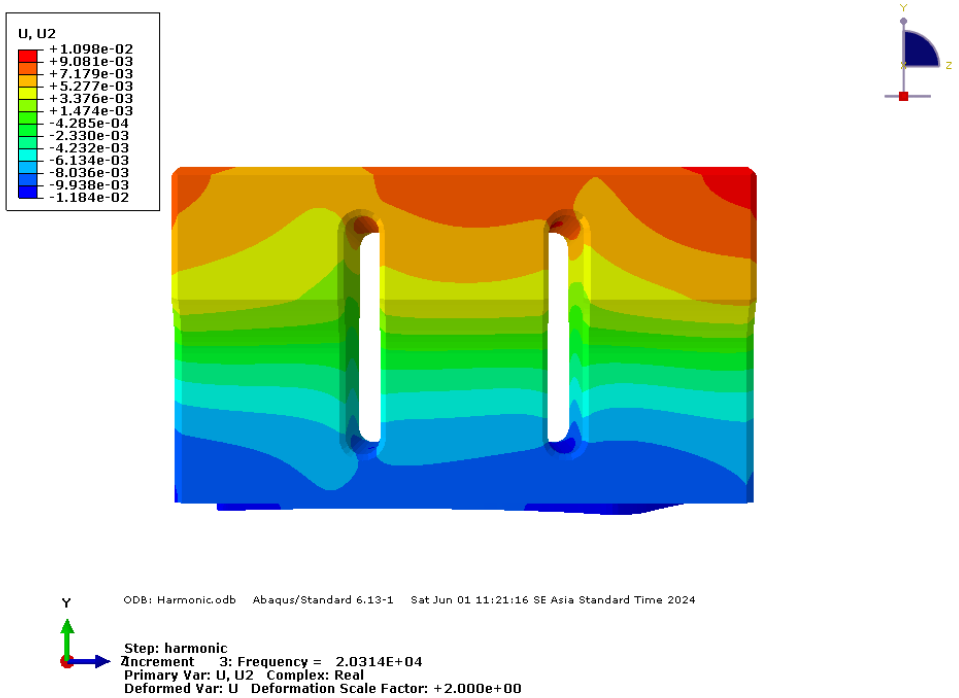


Fig. 9. Displacment analysis of T12 design

It is noticed that evaluating displacement of the whole horn body is beyond the scope of this study. The amplitude uniformity in the working surface is evaluated by a proposed parameter, namely Displacement unevenness ($\alpha$). This is defined as the absolute value of the difference between the maximum and minimum displacements in the working surface of the block horn. Hence, the larger the absolute value of the difference between the largest displacement and the smallest displacement, the higher the unevenness:

$$\alpha = |u_{max} - u_{min}| \quad (2)$$

Where: $u_{max}$, and $u_{max}$ are the maximum and minimum value of displacement calculated in absolute value.

The displacements of the points in the working surface of the designed horns described as in Fig 10. The displacements of the of the points in the working surface of T12 design are horizontally developed as showed in Fig 11. In term of the algebraic value, the maximum displacement on the working surface profile is -9.22 μm, while the minimum displacement is -11.5 μm.

Hence, Displacement unevenness is as follows:

$$\alpha = |-9.22 - (-11.5)| = 2.28\ \mu m$$

Do the same process, it is obtained Displacement unevenness for T17 and T20 designs are 2.6 μm and 40.9 μm respectively. Based on these results, it can be concluded that an increase in the width slots leads increase in Displacement unevenness or the unevenness of apmlitude in the working surface.

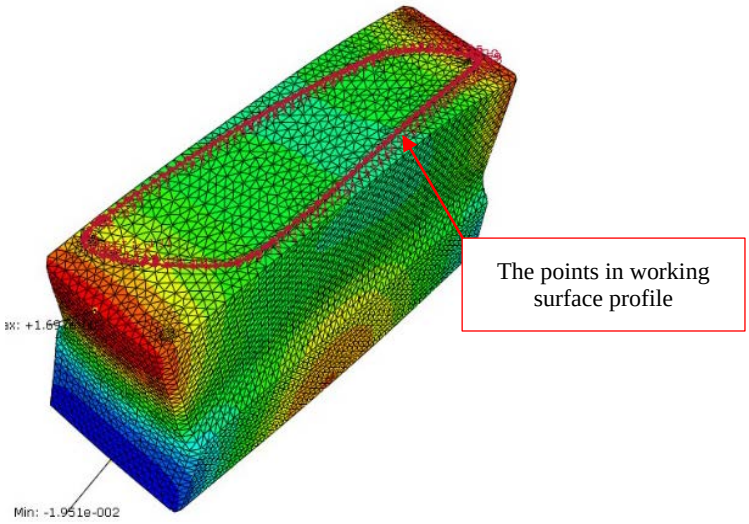


Fig. 10. Points selected for determining the displacements on the weld tip profile

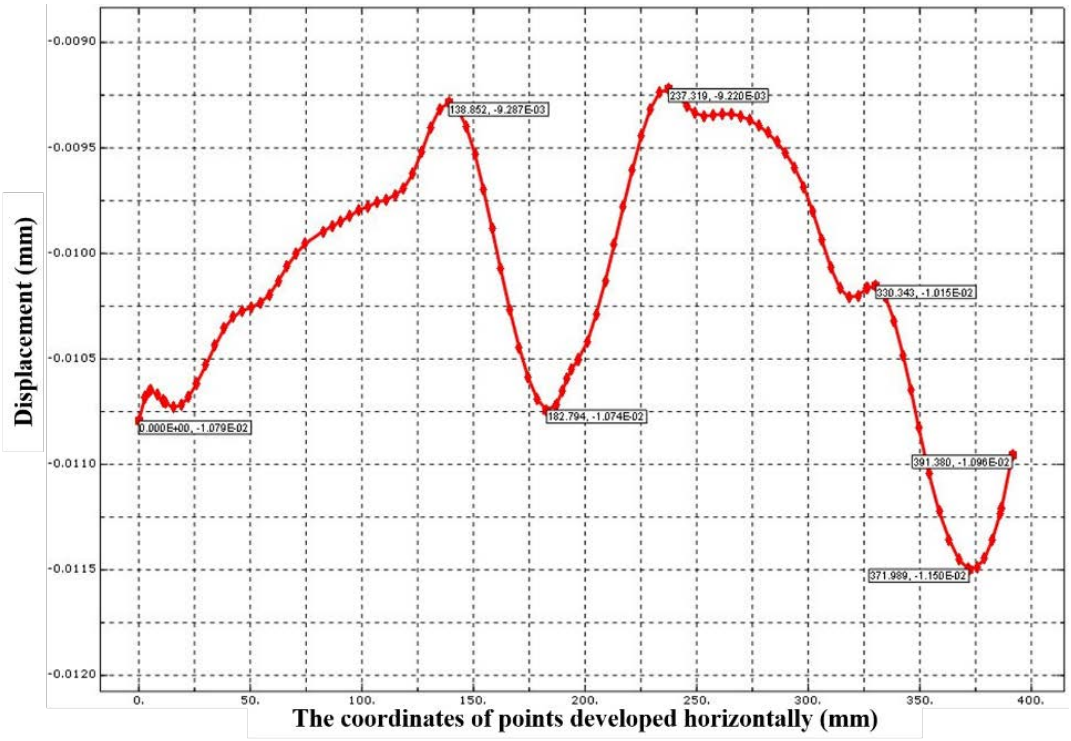


Fig. 11. Displacement of points on the working profile surface of T12 design

Fig12 gives qualitative information on the stress generated in the horn body of the T12 design. The maximum stress value is concentrated in the connection between the upper and lower body of the horn because of the change in cross-section. This phenomenon causes the stress concentration in this location. The stress at points on the working surface extracted from the results of ABAQUS has an absolute value of magnitude close to zero. This is beneficial for design because during work the contact between the working surface and the work-piece does not cause damage at these points. The stress distribution as shown in the Fig ensures uniform strength in the weld head structure.

Similar results were also observed in the case of two remaining designs, e.g. T17 and T20.

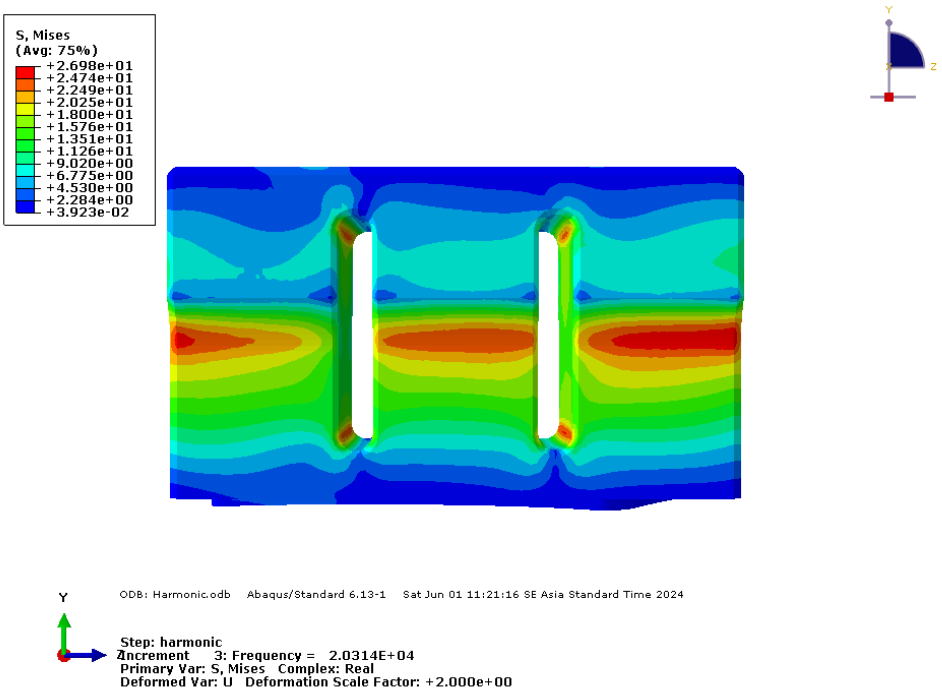


Fig. 12. Stress analysis of T12 design

For a more thorough evaluation of the output differences of the three designs, stresses and displacements of 120 points on the working surface are extracted. The ABAQUS partition technique is utilized to ensure that the positions of these 120 points are the same across the three designs. The average stress, and displacement (with standard deviation) values of the points mentioned above are used to evaluate the design for three designs of T12, T17, and T20. Fig 13 shows the mean values of displacements of 120 selected points along the working surface for the three designs. The results show that the T12 welding surface produces the largest mean displacement (10.2 μm) and the smallest standard deviation (0.63 μm). The small value of the standard deviation indicates that the uniformity of the displacement on the weld profile is the best. In contrast, the T20 tip produces the smallest mean displacement (4.38 μm) and the largest standard deviation (4.13 μm). This confirms that the displacement variation on the weld profile is large. These results are consistent with the results previously analyzed.

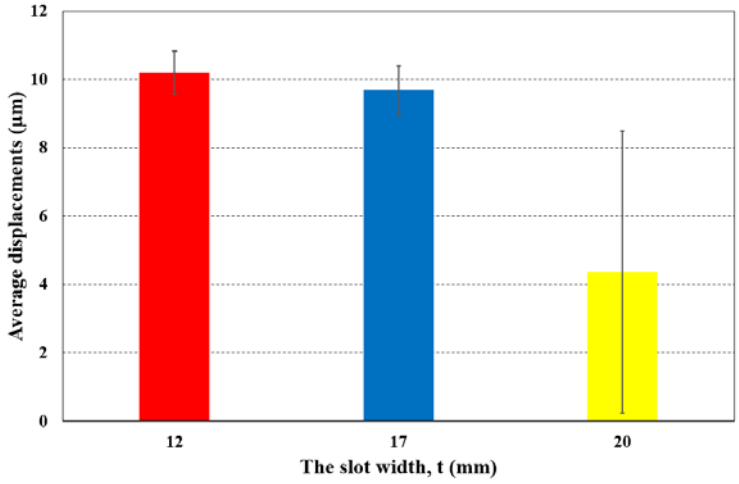


Fig. 13. Average displacement of 120 points on the working surface profile

The stress distributions obtained from the harmonic analysis of the three designs indicate qualitatively that the stresses near or on the weld profile are minimal in absolute value. For a more precise assessment, the mean stress and standard deviation of all three designs will be considered as shown in Fig 14. Small stress on the tip profile will be safe when the tip is in contact with the welded parts [9]. It can be seen that the T17 design produces the smallest average stress (0.09 Mpa). In addition, the standard deviation of the average stress value on T17 is 0.1 Mpa, also reaching the smallest value. In contrast, the T20 design produces the largest average stress value, as well as the most stress heterogeneity shown by the largest value of the standard deviation (0.36 Mpa).

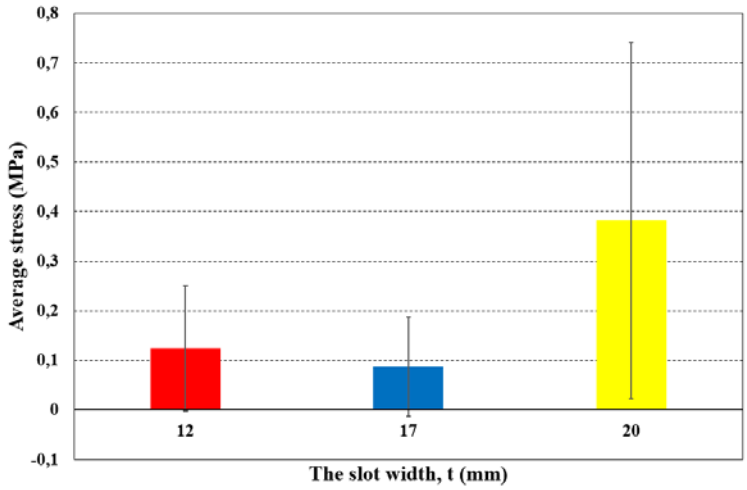


Fig. 14. Average stress of 120 points on the working surface profile

From the above analysis results, it can be seen that the T20 design produces outputs that do not satisfy the requirements such as displacement uniformity and unevenly distributed stress on the welding horn. Meanwhile, designs T12 and T17 satisfy both of the above criteria, especially design T17. Although the T17 design produces higher mean displacement amplitudes and displacement nonuniformities than the corresponding values of the T12 design, the natural frequency is closer to the target operating frequency. In addition, the T17 design creates smaller and more uniform stresses on the weld profile than the T12 design. Therefore, within the scope of this paper, it can be concluded that the design of the welding head with a complex profile with a 17 mm wide groove is considered to be the optimal design to achieve the requirements of the welding head. In addition to the groove width, in practice it is possible that the interaction between the dimensional parameters of the solder tip can affect the output requirements. Therefore, for a more optimal design, a larger-scale optimization problem should be considered in the future.

## 4 CONCLUSIONS

In this study, for the first time a block horn with a complex surface profile used for welding plastic turn signal cars was designed. FEM is used to analyze and simulate designs. The influence of the slot width on the performance of the horn was evaluated. The effectiveness of the design is shown through two output parameters: displacement uniformity on the working surface profile and stress distribution arising inside the structure. In order to quantify the uniformity of the working surface with complex profile, a new parameter, Displacement unevenness ($\alpha$), is proposed. The results show that slot width has an influence on the output requirements of the design. Of the three designs selected, the T20 design does not guarantee the output requirements. Meanwhile, the T17 design relatively balances the output requirements and can be considered an optimal design within the scope of the article. The results obtained by this study can be considered preliminary for further studies of designing ultrasonic horns having complicated working surface. Although the results of the article also have certain new contributions, to further develop the research results, some of the following issues need to be further researched in the future.

- To confirm the reliability of the FEA model proposed by the article, experimental research needs to be used to verify the results.
- In order to obtain an optimal design for welding horns with complex profiles, the influence of dimensional parameters such as geometry such as slot width (t), slot length (l), distance from the tip top to slot (s), upper body thickness ($t_1$), lower body thickness ($t_2$), fillet radius should be evaluated simultaneously.

## 5 ACKNOWLEDGEMENT

This research was funded by the Vietnam Ministry of Education and Training, grant number B2023-TNA-18

## 6 REFERENCES

[1] Rezaei, M., Farzin, M., Ahmadi, F., & Niroomand, M. R. (2022). Design, Analysis and Manufacturing of a Bone Cutting Ultrasonic Horn-Tool and Verification with Experimental Tests. Journal of Applied and Computational Mechanics, 8(2), 438-447. doi: 10.22055/jacm.2020.31298.1904

[2] Mubashir, M., Mutahir, R., & Shoaib Ur Rehman, M. (2022). Design and Analysis of Hollow Catenoidal Horn Profile for Ultrasonic Machining of Composite Materials. Journal of Studies in Science and Engineering, 2(2), 18–32. https://doi.org/10.53898/josse2022222

[3] Al Sarraf, Z., & Abdullah, Z. (2022). Design Optimization of Two Diagonal Slotted Block Horn for Ultrasonic Plastic Welding. International Journal Of Advanced Research In Engineering Innovation, 4(4), 70-83. https://doi.org/10.55057/ijarei.2022.4.4.7

[4] Roopa, R. M., Prakasan, K., & Rudramoorthy, R. (2008). Studies on High Density Polyethylene in the Far-field Region in Ultrasonic Welding of Plastics. Polymer-Plastics Technology and Engineering, 47(8), 762–770. https://doi.org/10.1080/03602550802188649

[5] Naď, M. (2010). Ultrasonic horn design for ultrasonic machining technologies. Applied and Computational Mechanics, 4(1), 79 – 88.

[6] Sooriyamoorthy, E., John Henry, S.P. & Kalakkath, P. (2011). Experimental studies on optimization of process parameters and finite element analysis of temperature and stress distribution on joining of Al–Al and Al–Al2O3 using ultrasonic welding. Int J Adv Manuf Technol, 55 (5-8), 631–640. https://doi.org/10.1007/s00170-010-3059-7

[7] Nguyen, Thanh-hai, Le Quang Thanh, Nguyen Huu Loc, Manh Ngo Huu, and Anh Nguyen Van. (2020). Effects of Different Roller Profiles on the Microstructure and Peel Strength of the Ultrasonic Welding Joints of Nonwoven Fabrics. Applied Sciences, 10, 12: 4101. https://doi.org/10.3390/app10124101

[8] Shuyu Lin, Hao Guo, Jie Xu. (2018). Actively adjustable step-type ultrasonic horns in longitudinal vibration. Journal of Sound and Vibration, 419, 367-379. https://doi.org/10.1016/j.jsv.2018.01.033

[9] Kothuru, V. V. L. ., Sistla, V. S. ., Mohammed, I. H. ., & Jagana, A. (2022). Design and Numerical Analysis of Rectangular Sonotrode for Ultrasonic Welding. Trends in Sciences, 19(11), 4215. https://doi.org/10.48048/tis.2022.4215

[10] P. K. J and P. K. (2018). Acoustic horn design for joining metallic wire with flat metallic sheet by ultrasonic vibrations. Journal of Vibroengineering, 20 (7), 2758–2770. https://doi.org/10.21595/jve.2018.19648

[11] Shahid, M.B., Jung, JY. & Park, DS. (2020). Finite element analysis coupled artificial neural network approach to design the longitudinal-torsional mode ultrasonic welding horn. Int J Adv Manuf Technol, 107, 2731–2743. https://doi.org/10.1007/s00170-020-05200-5

[12] Mehran Afshari, Behrooz Arezoo. (2021). Optimal design and experimental validation of ultrasonic wide blade horn. Applied Acoustics, 182. https://doi.org/10.1016/j.apacoust.2021.108254

[13] Andrea Cardoni, Margaret Lucas. (2002). Enhanced vibration performance of ultrasonic block horns. Ultrasonics, 40 (1-8), 365-369. https://doi.org/10.1016/S0041-624X(02)00123-3

[14] G. Graham, J.N. Petzing, M. Lucas. (1999). Modal analysis of ultrasonic block horns by ESPI. Ultrasonics, 37 (2), 149-157. https://doi.org/10.1016/S0041-624X(98)00050-X

[15] Lucas, M., and Smith, A. C. (1997). Redesign of Ultrasonic Block Horns for Improved Vibration Performance. ASME. J. Vib. Acoust, 119(3), 410–414. https://doi.org/10.1115/1.2889739

[16] S. -R. Kim, J. H. Lee, C. D. Yoo, J. –Y. (2011). Design of highly uniform spool and bar horns for ultrasonic bonding. IEEE Transactions on Ultrasonics, Ferroelectrics, and Frequency Control, 58(10), 2194-220. doi: 10.1109/TUFFC.2011.2069

[17] M. Roopa Rani, R. Rudramoorthy. (2013). Computational modeling and experimental studies of the dynamic performance of ultrasonic horn profiles used in plastic welding. Ultrasonics, 53(3), 763-772. https://doi.org/10.1016/j.ultras.2012.11.003

[18] Liesegang, M.; Yu, Y.; Beck, T.; Balle. F .(2021). Sonotrodes for Ultrasonic Welding of Titanium/CFRP-Joints—Materials Selection and Design. J. Manuf. Mater. Process, 5, 61. https://doi.org/10.3390/jmmp5020061

[19] Derks, P. (1984). The design of ultrasonic resonators with wide output cross-sections. The design of ultrasonic resonators with wide output cross-sections. Ph. D. Dissertation, Technische Hogeschool, Eindhoven, Netherlands.

[20] Kumar, R. D., Rani, M. R., & Elangovan, S. (2014). Design and Analysis of Slotted Horn for Ultrasonic Plastic Welding. Applied Mechanics and Materials, 592–594, 859–863. https://doi.org/10.4028/www.scientific.net/amm.592-594.859

[21] Anand K, Elangovan S. (2023). Design optimization of block horn for ultrasonic joining application using RSM–FEA–GA integration approach. Proceedings of the Institution of Mechanical Engineers, Part E: Journal of Process Mechanical Engineering, 237(6), 2429-2439. doi:10.1177/09544089221136801

[22] Afshari, M., & Arezoo, B. (2021). Design of wide ultrasonic horns based on topology optimization. Engineering Optimization, 54(6), 907–927. https://doi.org/10.1080/0305215X.2021.1901285

[23] Afshari, M., & Arezoo, B. (2022). A new design of wide blade ultrasonic horns using Non-Uniform Rational B-Spline shaped slots. Applied Acoustics, 196. https://doi.org/10.1016/j.apacoust.2022.108871

[24] Tanlak N, Sonmez F, Talay E. (2011). Detailed and simplified models of bolted joints under impact loading. The Journal of Strain Analysis for Engineering Design, 46(3), 213-225. doi:10.1177/0309324710396997

*Paper submitted: 04.06.2024.*

*Paper accepted: 06.11.2024.*